Quantum search in many-body interacting systems with long-range interactions

Fan Xing, Yan Wei, and Zeyang Liao*

State Key Laboratory of Optoelectronic Materials and Technologies, School of Physics, Sun Yat-sen University, Guangzhou 510275, China

(Received 15 January 2024; revised 29 March 2024; accepted 10 May 2024; published 23 May 2024)

Continuous-time quantum walks provide an alternative method for quantum search problems. Most earlier studies confirmed that quadratic speedup exists in some synthetic Hamiltonians, but whether there is quadratic speedup in real physical systems remains elusive. Here, we investigate three physical systems with long-range atom-atom interaction which are possibly good candidates for realizing the quantum search, including one-dimensional atom arrays either trapped in an optical lattice or coupled to a waveguide near the band edge or dispersively coupled to a good cavity. We find that all three systems can provide a near-optimal quantum search if there is no dissipation. However, if the dissipation is considered, only the latter two systems (i.e., waveguide-QED and cavity-QED systems) can still have high success probabilities because they can significantly enhance the atom-atom interaction even if they are far apart and the spectra gap can be much larger, which can reduce the search time and the effects of dissipation significantly. Our studies here can provide helpful instructions for realizing quantum search in real physical systems in the noisy intermediate-scale quantum era.

DOI: 10.1103/PhysRevA.109.052435

I. INTRODUCTION

Spatial search, the problem of finding a marked node in a graph, is one of the most widely used algorithms and can be applied to search engines, combinatorial optimization (path navigation, recommendation systems), new materials and drug discovery, and many other mathematical problems (including independent sets, satisfiability problem (SAT), dissimilar elements, subgroup finding, local search, and weight determination) [1,2]. For classical search algorithms, no shortcut is known, and $O(n)$ queries are typically required, where n is the total number of elements. Quantum computation promises computational speedup over certain types of problems by leveraging quantum properties such as quantum superposition and entanglement [1]. Grover first proposed a quantum search algorithm that requires only $O(\sqrt{n})$ oracle operations [3–5], and this algorithm can be realized based on the quantum circuit model, which has attracted extensive interest [6–8]. In addition to solving search problems, the quantum search algorithm also provides new insight into ground-state preparation [9,10], high-energy-physics data processing [11], optimization problems [12,13], and cryptography [14], as well as solving NP-hard problems [15,16].

In addition to the quantum circuit model, quantum computation can also be implemented via Hamiltonian evolution, such as quantum adiabatic evolution [17–20] and quantum random walks [21–27]. In 1998, Farhi and Gutmann proposed a quantum search algorithm based on continuous-time Hamiltonian evolution, and they showed that quadratic speedup can also be achieved in a complete graph (i.e., every vertex has the same nonvanishing hopping rate as all other vertices) [28]. It was then shown that for a hypercube graph in which two vertices are connected with equal strength if and only if they differ in a single bit, the quantum spatial search algorithm based on Hamiltonian evolution can also provide a quadratic speedup [29]. Based on a quantum analog of a discrete-time random walk (DTRW), Shenvi *et al.* also showed that optimal search can be achieved in a hypercube graph [30]. In contrast to the DTRW algorithm, Childs and Goldstone proposed that spatial search can also be constructed via a continuous-time quantum walk (CTQW); they showed that for a periodic lattice with dimension $d > 4$ the marked node can be found in the optimal $O(\sqrt{n})$ time, while $O(\sqrt{n}\log^{\frac{3}{2}} n)$ running times are required for $d = 4$ [31]. However, for $d < 4$ they showed that quadratic speedup is impossible. After that, many works showed that spatial search using a CTQW is also optimal for other graph topologies, such as fractal graphs [32], nonregular graphs [33], Erdös-Rényi graphs [34], and various network systems [35–37]. In recent years, the necessary and sufficient conditions that a graph must fulfill for optimal quantum search have attracted intensive studies [38–42].

In most of the previous studies, the quantum search algorithms were designed for pure mathematical models in which the hopping rate is usually assumed to be a distance-independent constant and the dissipation of the system is usually ignored. In 2014, Childs and Ge showed that if the interaction strength decays as a quadratic power law with distance, the optimal spatial search can still be obtained in a dimension $d = 2$ system [43]. In 2021, Lewis *et al.* studied the spatial search on a closed one-dimensional (1D) spin chain with long-range interactions, where the system Hamiltonian $H_0 = \sum_{i<j} J_{ij}(|i\rangle\langle j| + |j\rangle\langle i|)$, with $J_{ij} = |j-i|^{-\alpha} + |n-(j-i)|^{-\alpha}$, and they showed that the optimal spatial search exists when $\alpha < 1.5$ but does not exist when $\alpha > 1.5$ [44]. Although this type of interaction may, in principle, be implemented in the linear ion-trap-chain system with a single-band Mølmer-Sørensen scheme [45,46], its practical realization is challenging.

*Corresponding author: liaozy7@mail.sysu.edu.cn

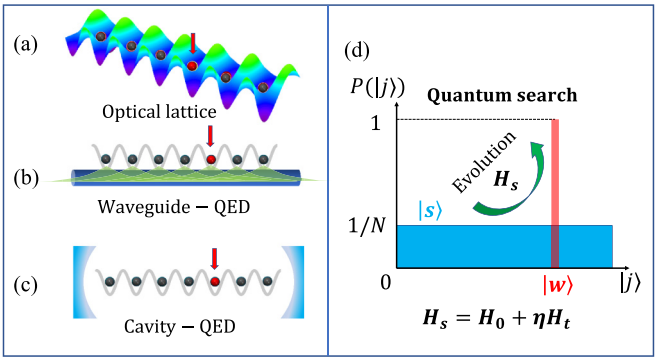

FIG. 1. Quantum search in three different physical systems: (a) 1D cold-atom array trapped in an optical lattice with a mixture of power-law interaction between atoms, (b) 1D atom array coupled to a waveguide with an exponentially decaying interaction between atoms, and (c) 1D atom array dispersively coupled to a cavity with ideal long-range interactions between atoms. (d) Schematic diagram of the quantum search algorithm where the system evolves from an equal superposition state $|s\rangle$ to the target state $|w\rangle$ under the evolution of search Hamiltonian H_s.

In this paper, we study the quantum search on three physical systems with different long-range interactions, and the aim is to find a physical realization as close as possible to the quantum search on the complete graph, which is known to be optimal [31]. The three physical systems we investigate include an atom chain either trapped in an optical lattice, coupled to a 1D photonic waveguide near the photonic band edge, or dispersively coupled to a high-quality cavity. The results show that quadratic speedup with high success probability can be approached in all three systems if the dissipation is ignored. However, if the dissipation is considered, the success probability in the first system is extremely low, while the waveguide-QED and cavity-QED systems can still provide relatively high success probabilities due to the significant enhancement of collective long-range atom-atom interaction and the reduction of dissipation effects via vacuum engineering. Our findings can provide helpful instructions for the experimental realization of the quantum spatial search in the noisy intermediate-scale quantum (NISQ) era [47].

This paper is organized as follows. In Sec. II we discuss the three different physical models and the quantum search algorithm based on CTQW. Then we numerically calculate the quantum search on the three different physical systems and show the condition for quadratic speedup over the classical search without dissipation noises in Sec. III and with dissipation noises in Sec. IV. Finally, we summarize our results.

II. MODEL AND THEORY

A. Physical model

Here, we consider the quantum search in a 1D atom array coupled to three photonic baths, i.e., a free-space optical lattice and waveguide-QED and cavity-QED systems, as shown in Fig. 1. We assume that all the atoms are identical and have the same transition angular frequency ω_a, and their nearest-neighbor separation is d. The atom-atom interaction can be long range in all three systems, but how the interactions depend on the atom separation is quite different in these three systems. In a photonic environment, the electric field at position $\vec{r}$ generated by a dipole $\vec{\mu}_1$ at position $\vec{r}_0$ with oscillation frequency ω is given by $\vec{E}(\vec{r}) = \omega^2\mu\vec{G}(\vec{r},\vec{r}_0,\omega)\cdot\vec{\mu}_1$, where μ is the permeability of the photonic bath and $\vec{G}(\vec{r},\vec{r}_0,\omega_a)$ is the dyadic Green's function of the photonic environment [48]. When another dipole, $\vec{\mu}_2$, with the same oscillation frequency is placed in position $\vec{r}$, the dipole-dipole coupling energy is then given by $\vec{\mu}_2\cdot\vec{E}(\vec{r}) = \omega^2\mu\vec{\mu}_2\cdot\vec{G}(\vec{r},\vec{r}_0,\omega)\cdot\vec{\mu}_1$. Thus, the general expression for the effective atom-atom interaction in an arbitrary photonic bath is then given by [49]

$$V_{ij} = J_{ij} + i\Gamma_{ij}/2 = \left(\omega_a^2\mu/\hbar\right)\vec{\mu}_i^*\cdot\vec{G}(\vec{r}_i,\vec{r}_j,\omega_a)\cdot\vec{\mu}_j, \quad (1)$$

where the real part J_{ij} is the coherent dipole-dipole interaction and the imaginary part Γ_{ij} is the incoherent collective dissipation rate mediated by the photonic baths. $\vec{\mu}_i^*$ is the transition dipole moment of the ith atom at position $\vec{r}_i$ which is assumed to be perpendicular to the atom arrays, and $\hbar$ is the reduced Planck constant. The effective atom-atom interactions and the collective decays for the three cases are shown in Table I. Before proceeding, we first introduce the definition of the so-called long-range interaction used in the current work. Here, "long range" is used to denote generic nonlocal couplings, i.e., beyond on-site or nearest-neighbor couplings [50].

For an atom array trapped by a 1D optical lattice, the atom-atom interaction is a mixture of power-law interaction, i.e., $J_{ij} = \frac{3\gamma}{4}[-\frac{\cos(k_a r_{ij})}{k_a r_{ij}} + \frac{\sin(k_a r_{ij})}{(k_a r_{ij})^2} + \frac{\cos(k_a r_{ij})}{(k_a r_{ij})^3}]$ and the collective decay $\Gamma_{ij} = \frac{3\gamma}{2}[\frac{\sin(k_a r_{ij})}{k_a r_{ij}} + \frac{\cos(k_a r_{ij})}{(k_a r_{ij})^2} - \frac{\sin(k_a r_{ij})}{(k_a r_{ij})^3}]$, where γ is the spontaneous decay rate of a single atom in the free space, $k_a = \omega_a/c$ (c is the speed of light), and $r_{ij} = |\vec{r}_i - \vec{r}_j|$ [51,52]. When $r_{ij} \gg \lambda_a$ (λ_a is the wavelength related to ω_a), $J_{ij} \propto 1/r_{ij}$, $\Gamma_{ii} \to \gamma$, and $\Gamma_{ij} \to 0$ when $i \neq j$. If the power-law interaction decays as $1/x^\alpha$, it can be called strong long-range interaction when $\alpha < d$ and weak long-range interaction when $\alpha > d$, where d is the dimension of the system according to Ref. [50].

For the atom-waveguide coupling system, the effective atom-atom interaction in the case when the atomic transition frequency is above the cutoff frequency of the waveguide is given by $V_{ij} = (\Gamma/2)e^{ik_a r_{ij}}$, where Γ is the decay rate into the waveguide mode [53–57]. The coherent part of the interaction is also long range, but it periodically varies with atom distance. If the atomic transition frequency is slightly below the cutoff frequency ω_c of the waveguide, the atom is mainly coupled to the modes around the band edge due to the Van Hove singularity of the density of states, and the radiation dissipation can be almost completely suppressed [58,59]. In this case, the effective atom-atom interaction is given by $V_{ij} = (\Gamma/2)e^{-\kappa r_{ij}}$, which exponentially decays as the atom separation increases with decay factor $\kappa = \sqrt{\omega_c^2 - \omega_a^2}/c$ [60,61]. Although it decreases exponentially with atom separation, the effective coupling length depends on the detuning $\Delta = \omega_c - \omega_a$, which can still become effective long range if the detuning is very small. For example, if κ is very small, there is still a significant interaction between the first and last atoms which is a long-range interaction according to the definition of long range used in the current work. The advantage of the case when the atomic transition is below the

TABLE I. Coherent atom-atom interaction strengths and incoherent dissipation for different physical systems with long-range interaction.

Physical system	Coherent interaction	Collective dissipation
Free-space optical lattice	$J_{ij}=\frac{3\gamma}{4}\left[-\frac{\cos(k_a r_{ij})}{k_a r_{ij}}+\frac{\sin(k_a r_{ij})}{(k_a r_{ij})^2}+\frac{\cos(k_a r_{ij})}{(k_a r_{ij})^3}\right]$	$\Gamma_{ij}=\frac{3\gamma}{2}\left[\frac{\sin(k_a r_{ij})}{k_a r_{ij}}+\frac{\cos(k_a r_{ij})}{(k_a r_{ij})^2}-\frac{\sin(k_a r_{ij})}{(k_a r_{ij})^3}\right]$
Waveguide QED above the band gap	$J_{ij}=\frac{\Gamma}{2}\sin(k_a r_{ij})$	$\Gamma_{ij}\to\frac{\Gamma}{2}\cos(k_a r_{ij})$
Waveguide QED within the band gap	$J_{ij}=\frac{\Gamma}{2}e^{-\kappa r_{ij}}$	$\Gamma_{ij}\to 0$
Cavity QED with dispersive coupling	$J_{ij}=\frac{g^2}{\Delta}$	$\Gamma_{ij}\approx\frac{3\gamma}{2}\left[\frac{\sin(k_a r_{ij})}{k_a r_{ij}}+\frac{\cos(k_a r_{ij})}{(k_a r_{ij})^2}-\frac{\sin(k_a r_{ij})}{(k_a r_{ij})^3}\right]$

cutoff frequency is that the spontaneous decay can be almost completely inhibited.

For the atom-cavity coupling system, we consider the case in which multiple two-level atoms dispersively couple to a common cavity mode which can produce effective infinite long-range interaction between atoms $J_{ij}^C=g^2/\Delta$, where g is the atom-cavity coupling strength and Δ is the detuning between the atomic transition frequency and the cavity frequency [62]. It is clearly seen that the atom-atom interaction in this case is effectively infinitely long range and does not decrease with atom distance. Since the atomic transition frequency is significantly detuned from the cavity mode, the dissipation to the cavity mode is largely suppressed, but the dissipation in other directions can still occur, and therefore, the dissipation is about the same as that in the free space, as shown in Table I [63].

B. Quantum search based on CTQW

Considering that there are n atoms with a single excitation in the above systems, they can be mapped to a graph G with n vertices, each representing a single excited atom. The basis state $|j\rangle=|0\cdots 1_j\cdots 0\rangle$, with $j=1,2,\ldots,n$ denoting that the jth atom is in the excited state while other atoms are in the ground state. According to the continuous-time quantum walk spatial search algorithm proposed by Childs and Goldstone [31], we can construct the search Hamiltonian

$$H_s=H_0+\eta H_t. \tag{2}$$

Here, $H_0=\sum_{ij}V_{ij}\sigma_{eg}^i\sigma_{ge}^j$ is the effective system (graph) Hamiltonian in the interaction picture, and V_{ij} is the effective coupling strength given by Eq. (1); detailed expressions of V_{ij} for the three different physical systems are shown in Table I. $\sigma_{eg}^i=|e\rangle_i\langle g|$, and $\sigma_{ge}^j=|g\rangle_j\langle e|$, so H_0 can be written as $H_0=\sum_{ij}V_{ij}|i\rangle\langle j|$. $H_t=|w\rangle\langle w|$ is the target-state Hamiltonian, with $w\in\{1,\ldots,n\}$ denoting that the wth atom is excited and other atoms are in the ground state and parameter η denoting the relative strength of the two Hamiltonians. In practical realizations, the target Hamiltonian is realized by shifting the transition frequency of the wth atom by applying an external control field. Here, we should mention the connection between our search Hamiltonian in Eq. (2) and the search Hamiltonian used in previous research, i.e., $H_s=\beta H_0+H_t$, where $H_0=\sum_{ij}|i\rangle\langle j|$ without dissipation [31]. In the case of the complete graph without dissipation, i.e., J_{ij} is a constant (e.g., $J_{ij}=J_0$), it is readily seen that when $\eta=J_0/\beta$, the two Hamiltonians are actually equivalent and differ by only a constant rescaling factor.

The typical initial state of the system is an equal superposition of one excitation state, i.e., $|s\rangle=\frac{1}{\sqrt{n}}\sum_{j=1}^n|j\rangle$. For a quantum search algorithm, we require that the system can evolve to the target state $|w\rangle$ with high fidelity at a certain time under the Hamiltonian in Eq. (2). If the atom-atom interaction is ideally long range and J_{ij} is a positive constant, it is not difficult to prove that $|s\rangle$ is the eigenstate of the coherent part of H_0 with the largest eigenvalue. When $\eta\to\infty$, $|w\rangle$ is the eigenstate of H_s with the largest eigenvalue. At certain finite values of η, neither the $|s\rangle$ nor $|w\rangle$ state, but their superposition, is the eigenstate of H_s. We need to find the optimal value of η such that the relevant eigenstates have maximum overlap with both the $|s\rangle$ and $|w\rangle$ states. Under this condition, the system can oscillate between the $|s\rangle$ and $|w\rangle$ states, and at certain time, the system can evolve from the initial state $|s\rangle$ to the target state $|w\rangle$ with high fidelity.

The goal of the quantum search is to obtain the target state $|w\rangle$ from the initial state $|s\rangle$ with maximum fidelity, and the search procedure is as follows [31]. (1) Choose optimal η: Select an appropriate range of η to calculate the eigenvalues E_j and eigenstates $|\phi_j\rangle$ of the coherent part of H_s. Here, we mainly care about the eigenstates $|\phi_0\rangle$ and $|\phi_1\rangle$ with the largest and second-largest eigenvalues, i.e., E_0 and E_1. If η varies from zero to infinity, $|\phi_0\rangle$ switches from $|s\rangle$ to $|w\rangle$, and at a certain value of η the two eigenstates $|\phi_0\rangle$ and $|\phi_1\rangle$ cross, and these two eigenstates can both have substantial overlap on both $|s\rangle$ and $|w\rangle$. The crossover occurs under the condition that $\Delta E=E_0-E_1$ is the minimum from which we can determine the optimal parameter $\eta_{\rm opt}$. Under this Hamiltonian, the system can evolve from state $|s\rangle$ to the target state $|w\rangle$ with high fidelity at a time proportional to the inverse of the energy gap $\Delta T_{\rm min}=\pi/\Delta E_{\rm min}$. (2) To prove that the system can, indeed, evolve to the target state with high fidelity, we let the system evolve under the search Hamiltonian $H_s=H_0+\eta_{\rm opt}H_t$ from the initial state $|s\rangle$ for a time t, obtaining the final state $|\psi_f\rangle=e^{-iH_st}|s\rangle$. (3) Make a projection measurement; the success probability of finding the target state $|w\rangle$ is $F=|\langle w|e^{-iH_st}|s\rangle|^2$. Define the time corresponding to the maximum fidelity as the optimal search time $T_{\rm opt}=t_{F_{\rm max}}$ and compare this search time with $\Delta T_{\rm min}$. (4) Vary the system size n and repeat the above procedures to determine the search time as a function of n. Finally, we fit the curves and see whether there is a quadratic speedup or not.

III. QUANTUM SEARCH WITHOUT DISSIPATION-NUMERICAL SIMULATION

In this section, we numerically study the optimal search time for the three different interacting systems shown in Fig. 1. We assume that in all three cases, atom separation is $d=\lambda_a$, which is the wavelength corresponding to the atomic transition frequency ω_a. In the following calculations, we let

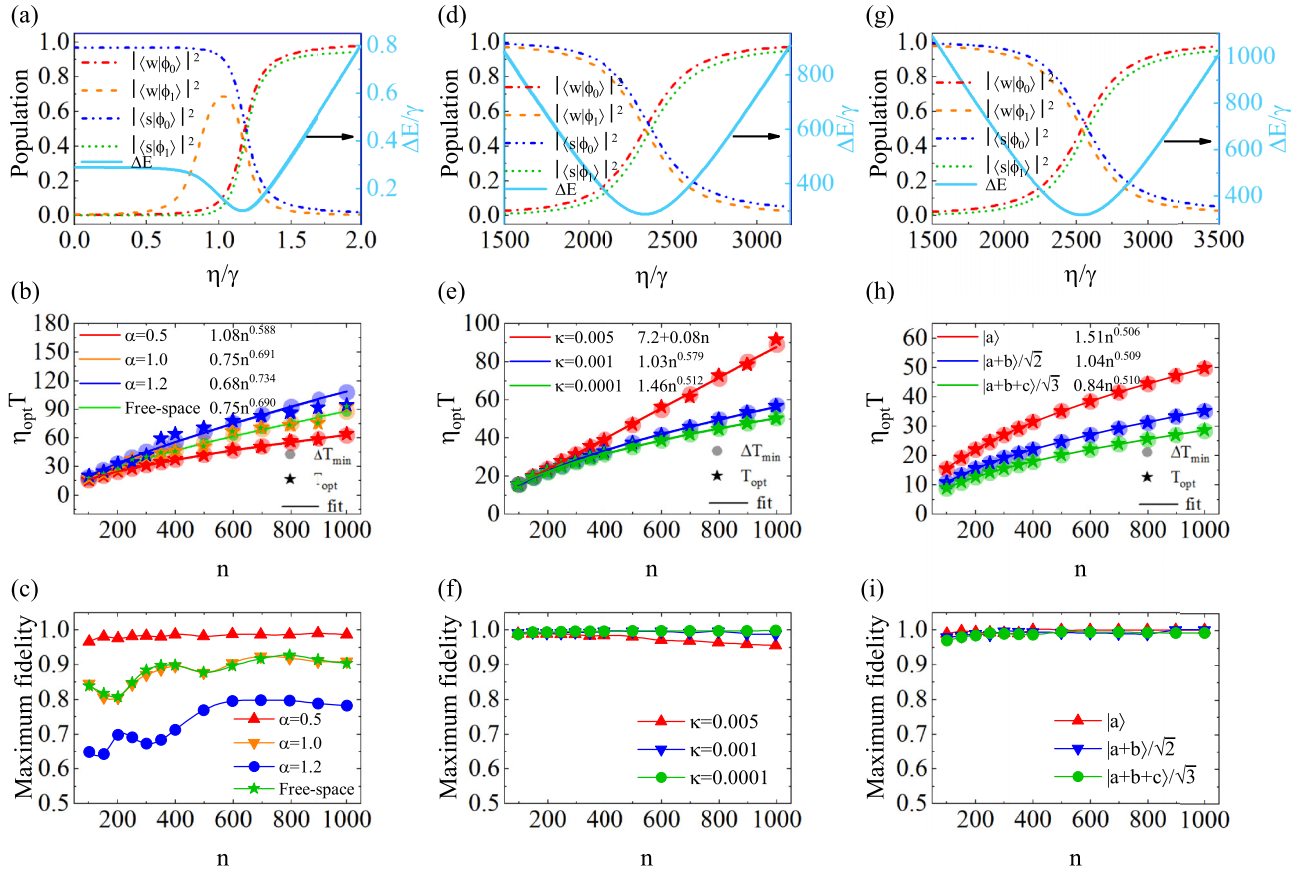

FIG. 2. The optimal η_{opt} for the three different physical systems: (a) an optical lattice, (d) a waveguide-QED system with $\kappa = 0.001$, and (g) a cavity-QED system. $n = 256$ for all three cases. Optimal search time and maximum fidelity for (b) and (c) mixed-power-law interaction in the free-space optical lattice and pure power-law interaction for $\alpha = 0.5, 1.0, 1.2$; (e) and (f) exponentially decaying interaction in the waveguide-QED system; and (h) and (i) infinite long-range interaction in the cavity-QED system.

$\lambda_a = 1$ for simplicity. Thus, the distance between the ith and jth atoms is given by $r_{ij} = |i - j|$. We vary the atom number from 100 to 1000 and calculate the search time for the three interaction systems using both ΔT_{min} and T_{opt}, as well as the maximum fidelity of finding the target state. To compare our results with the previous research on the ideal complete graph [31], we first ignore the dissipation of the system (i.e., $H_0 = \sum_{ij} J_{ij}|i\rangle\langle j|$) in this section; the effects of dissipation will be considered in the next section.

A. Atom array in an optical lattice: Multiple-power-law interaction

The spatial search on a closed 1D spin chain whose Hamiltonian $H_0 = \sum_{i<j} J_{ij}(|i\rangle\langle j| + |j\rangle\langle i|)$, with $J_{ij} = |j - i|^{-\alpha} + |n - (j - i)|^{-\alpha}$, has already been studied [44]. Here, we discuss a slightly different power-law interaction which may be much easier to implement. As is known to us, an atom array in the free space or trapped by an optical lattice can have dipole-dipole interaction induced by the free-space vacuum, which is a mixture of power laws, as shown in Table I [51,52]. When $k_a r_{ij} \gg 1$, $J_{ij} \propto r_{ij}^{-1}$, while when $k_a r_{ij} \ll 1$, $J_{ij} \propto r_{ij}^{-3}$. Since we mainly consider the case when the nearest-neighbor atom separation is λ_a, the atom-atom interaction J_{ij} is dominated by the first term proportional to r_{ij}^{-1}. Different from the symmetric Hamiltonian used in Ref. [44], there is no known analytical solution for the multiple-power-law interaction Hamiltonian, and here, we resort to numerical simulations.

We first calculate the eigenvalues and eigenvectors of the search Hamiltonian in Eq. (2) as η varies from 0 to ∞. Taking $n = 256$ and $w = 20$ as an example, the energy difference ΔE between the largest and second-largest eigenvalues as a function of η is shown in Fig. 2(a), from which we can see that there is a minimum energy gap. The wave function overlaps between the two eigenstates ($|\phi_0\rangle$ and $|\phi_1\rangle$); the initial state $|s\rangle$ and target state $|w\rangle$ are also shown in Fig. 2(a). We can clearly see that when ΔE is the minimum, the two largest eigenstates almost equally overlap with $|s\rangle$ and $|w\rangle$ states, which is the requirement for an optimal quantum search with high success probability. From this, we can determine that the optimal $\eta_{\text{opt}} \approx 1.17\gamma$ when $n = 256$ and $|w\rangle = |20\rangle$. Now, with different sizes of atom arrays, we first determine the optimal η_{opt} for each n and then numerically calculate the optimal search time T_{opt} by evolving the system under the search Hamiltonian in Eq. (2). The results are shown by the green solid stars in Fig. 2(b). To compare the search times on equal footing, we have multiplied the search time by η_{opt} to eliminate the effect of η_{opt}. In addition to calculating the search time using Hamiltonian evolution, we also evaluate the search time by simply calculating ΔT_{min} from the minimum energy gap, and the results are shown by the green dots in Fig. 2(b). We can clearly see that the search times calculated

using these two methods coincide very well. By fitting the dots (green solid line), we can find that $\eta_{\rm opt}t_{\rm opt} = 0.75n^{0.690}$, which is slightly slower than the quadratic acceleration of Grover's search algorithm but is faster than the classical search algorithm. For comparison, we also show the results of pure power-law interaction (i.e., $J_{ij} \propto r_{ij}^{-\alpha}$) with $\alpha = 0.5$, 1.0, and 1.2. We can see that as α decreases, the search time also decreases and approaches the quadratic acceleration. The result for $\alpha = 1$ is very close to our free-space case, which confirms that the first term in J_{ij} dominates when $d = \lambda_a$.

We also calculate the maximum fidelity of the evolving final state with the target state, and the results are shown in Fig. 2(c). For the multiple-power-law interaction in the free-space case, the fidelity is between 80% and 90% when the system size varies from 100 to 1000. This fidelity is high enough for practical realization. In the pure power-law case, when α decreases, the success probability of finding the target node increases. Particularly, when $\alpha = 0.5$, the fidelity is close to unity. Again, the success probability when $\alpha = 1.0$ is almost the same as that in our case.

B. Waveguide-QED system: Exponentially decaying interaction

It is known that the atom-atom interaction in the waveguide-QED system can also be long range. When the atom transition frequency is above the cutoff frequency of the single-mode optical waveguide, the coherent atom-atom interaction is given by $J_{ij} = (\Gamma/2)\sin(k_a r_{ij})$, and the collective dissipation $\Gamma_{ij} = (\Gamma/2)\cos(k_a r_{ij})$, both of which are periodic functions of the atom separation (see Table I) [53–57]. We find that under this Hamiltonian, the equal superposition state $|s\rangle$ is not an eigenstate of H_0, and the optimal quantum search cannot be found.

Instead, we consider the case in which the atomic transition frequency is slightly less than the cutoff frequency of the single-mode optical waveguide where the atom-atom interaction exponentially decays with the atom separation, i.e., $J_{ij} = (\Gamma/2)e^{-\kappa r_{ij}}$ with vanishing dissipation, which is presented in the third row of Table I [60,61]. Here, in the numerical simulations, we choose $\Gamma = 20\gamma$ and three different values of κ (i.e., $\kappa = 0.005, 0.001$, and 0.0001). We choose these three different values of κ to demonstrate the search time transitioning from the linear function of n to the approximate quadric function of n. The parameter κ depends on the transition frequency of the atom and the cutoff frequency of the waveguide, i.e., $\kappa = \sqrt{\omega_c^2 - \omega_a^2}/c \approx \sqrt{2\omega_a \Delta\omega_{ca}}/c$, where $\Delta\omega_{ca} = \omega_c - \omega_a$ is the energy difference between the cutoff frequency and the atom transition frequency [60,61]. In practical realizations, we can control the detuning $\Delta\omega_{ca}$ to tune the value of κ. It should be noted that we set $\lambda_a = 1$ in the current work, and therefore, $\kappa = 0.001$ is actually in units of $1/\lambda_a$. Then, we have $\Delta\omega_{ca} \approx \kappa^2\omega_a/2$. Supposing that $\lambda_a = 1$ μm, the atomic transition frequency $\omega_a = 6\pi \times 10^{14}$ Hz. Obtaining $\kappa = 0.001$ requires that the energy difference $\Delta\omega_{ca} \approx 3\pi \times 10^8$ Hz. The energy difference $\Delta\omega \approx 75\pi \times 10^8$ Hz results in $\kappa = 0.005$, and $\Delta\omega \approx 3\pi \times 10^6$ Hz yields $\kappa = 0.0001$.

In Fig. 2(d), we show the energy difference ΔE between the largest and second-largest eigenvalues of the search Hamiltonian as a function of η when $n = 256$ and $\kappa = 0.001$. From Fig. 2(d), we can see that there is a minimum energy gap ΔE occurring at $\eta_{\rm opt} \approx 2335\gamma$, where the corresponding eigenstates have significant overlaps with the initial state $|s\rangle$ and the target state $|w\rangle$ ($|w\rangle = |20\rangle$ in our numerical calculations). We note that the optimal value of η here is much larger than that used in the free-space optical lattice with the same number of atoms. There are two main reasons why $\eta_{\rm opt}$ is much larger here. First, due to the confinement of the photon field, the interaction strength between the atom and the photon can be much larger, which leads to a larger Γ. Second, when κ is small, the atom-atom interaction decays slower than that in the free space, which results in a much stronger atom-atom interaction even if two atoms are far apart. Due to these two factors, the energy scale of the system is much larger, which requires a much larger $\eta_{\rm opt}$ to observe the crossover behavior, and the minimum energy gap ΔE in this case is also 3 orders of magnitude larger than that in the free-space optical lattice. Actually, the large value of $\eta_{\rm opt}$ can also be predicted from previous studies on the complete graph because the system here can be well described by a complete graph when $\kappa \to 0$. It has been shown in the complete graph that the optimal search is reached when $\beta \approx 1/n$ [31], which corresponds to $\eta_{\rm opt} \approx n\Gamma/2$ in our case. Thus, the optimal value of η depends on both the number of atoms and the atom-atom interaction strength Γ. Here, we choose $\Gamma = 20\gamma$, and thus, $\eta_{\rm opt} \approx 10n\gamma$. Indeed, for the case with $n = 256$, when κ is reduced from 0.001 to 0.0001, $\eta_{\rm opt}$ increases from 2335γ to 2520γ, which is approaching the value of 2560γ in the complete graph.

After determining the optimal values of η for each n, we numerically evolve the system under the search Hamiltonian in Eq. (2) with three different values of κ. We can determine the optimal search time as a function of the number of atoms n, as shown in Fig. 2(e). Again, to compare the search times on equal footing, here, we also multiply the search time by $\eta_{\rm opt}$. By fitting the curves, we find that when $\kappa = 0.005$, the search time $\eta_{\rm opt}t_{\rm opt} \propto 0.08n$ is a linear function of the number of sites. Thus, there is no quadratic speedup over the classical search ($\eta_{\rm opt}t \propto 0.5n$), but the slope in our quantum search here is about 6 times smaller, which indicates the speedup of the search. However, when we decrease the value of κ, we find that the search time also decreases. When $\kappa = 0.001$, the search time $\eta_{\rm opt}t_{\rm opt} \approx 1.03n^{0.579}$, and when $\kappa = 0.0001$, the search time $\eta_{\rm opt}t_{\rm opt} \approx 1.46n^{0.512}$, which is apparently approaching the quadratic speedup and also very close to the optimal quantum search time predicted in the complete graph [$t_{\rm opt} \approx (\pi/2)n^{1/2}$] [31]. The maximum fidelity (i.e., the success probability) as a function of n is shown in Fig. 2(f), from which we can see that the fidelities for all three cases are very close to unity. Thus, quantum speedup is also possible if the atom array is coupled to the waveguide near the photonic band edge.

C. Cavity-QED system: Infinite long-range interaction

For an atom chain dispersively coupled to a cavity, the atom-atom interaction induced by the common cavity mode is ideally infinitely long range with $J_{ij} = g^2/\Delta$, which is a constant for an arbitrary pair of atoms [62]. Thus, this system is a possible physical realization of a quantum search in a complete graph. Here, in the numerical simulation, we

assume that $J_{ij} = 10\gamma$, which is experimentally achievable [64]. To determine the optimal parameter η, we also calculate the energy gap ΔE between the largest and second-largest eigenvalues of the search Hamiltonian when η varies from 0 to ∞. Again, we find that there is also a minimum energy gap when $\eta_{\rm opt} = 2540\gamma$ [for $n = 256$, $|w\rangle = |20\rangle$; Fig. 2(g)]. We can readily see that $\eta_{\rm opt}$ here is also very close to the value (2560γ) predicted by the previous studies on the complete graph [31]. Similar to that in the waveguide-QED system, $\eta_{\rm opt}$ here is also much larger than that in the free-space system due to the much larger long-range atom-atom interactions. We also find that the minimum energy gap is 3 orders of magnitude larger than that in the free-space case, which can significantly reduce the search time. Then we numerically evolve the system and calculate the optimal search time $\Delta T_{\rm min}$ and $T_{\rm opt}$ for three different target states; the results are shown in Fig. 2(h). The three target states include searching for a single node $|w\rangle = |a\rangle$ and superposition of two nodes $|w\rangle = \frac{1}{\sqrt{2}}(|a\rangle + |b\rangle)$ and three nodes $|w\rangle = \frac{1}{\sqrt{3}}(|a\rangle + |b\rangle + |c\rangle)$, with $a = 20$, $b = 40$, and $c = 60$ as an example. From Fig. 2(h), we can see that $\Delta T_{\rm min}$ and $T_{\rm opt}$ coincide with each other, and there is a clearly quadratic speedup for searching all three different target states. For a single marked node, by fitting the curve we can obtain $\eta_{\rm opt} t_{\rm opt} \approx 1.51 n^{0.506}$, which is very close to the theoretical predicted behavior $[t_{\rm opt} \approx (\pi/2) n^{1/2}]$ in the complete graph [31]. We also see that $\eta_{\rm opt} t_{\rm opt} = 1.04 n^{0.509}$ and $\eta_{\rm opt} t_{\rm opt} = 0.84 n^{0.510}$ for the cases with two and three marked nodes, respectively. It turns out that searching a superposition state is even faster than searching a single node because this kind of target state has a larger overlap with the initial state. For searching multiple nodes in a complete graph, it has been shown that the search time is given by $t = (\pi/2)\sqrt{n/k}$, where k vertices are marked [65]. According to this prediction, the search time is reduced by $1/\sqrt{k}$ when k nodes are marked compared with the case when only one node is marked. Indeed, our numerical results are consistent with this prediction. The optimal search time for one node here is about $1.51 n^{0.506}$. Accordingly, the optimal search times for $k = 2$ and $k = 3$ are predicted to be about $1.06 n^{0.506}$ and $0.86 n^{0.506}$, which are very close to our numerical results $1.04 n^{0.509}$ and $0.84 n^{0.510}$, respectively. The maximum fidelities (or success probabilities) for finding the target states for all three cases are close to 100%, as shown in Fig. 2(i).

In both the waveguide-QED system with $\kappa \to 0$ and the cavity-QED system with infinite long-range interaction, $\eta_{\rm opt}$ is required to be much larger than γ, which may pose a great challenge for the experimental realization of the quantum search algorithm in these two models. However, this requirement is not impossible. For example, in [66], researchers demonstrated the tuning of the transition frequency by more than 40 MHz in superconducting qubits, while its relaxation time was about 10 kHz. Another possible candidate is the Rydberg atom, whose Stark effect can be of the order of gigahertz, while its decay rate can be as low as kilohertz [67,68].

D. Boundary effects

In the previous sections, we assumed that the position of the target is at $w = 20$. For a complete graph such as in the cavity-QED system with infinite long-range interaction, the position of the target does not affect the search time. However, if the atom-atom interaction is not ideally infinite as in the multiple-power-law interaction and exponentially decaying interaction cases, the connectivity of each node is not the same, and thus, the location of the marked node may affect the search time. For example, the atoms close to the boundaries (e.g., the leftmost and rightmost ones) are the least interacting with the rest of the atoms, and the search time for these nodes is expected to be longer. To demonstrate this boundary effect, we calculate the search time and fidelity when different locations of nodes are selected in the cases of multiple-power-law interactions in a 1D optical lattice and exponentially decaying interactions in the waveguide-QED system within the band gap. Taking $n = 500$ as an example, we compare the results when $w = 1$, 50, 150, 250, 350, 450, and 499; the results are shown in Fig. 3. From Figs. 3(a) and 3(b), we clearly see that when the target node is close to the boundary, the search time is longer, which is consistent with the expected prediction. The corresponding search fidelities are shown in Figs. 3(c) and 3(d), from which we can see that the fidelity does not significantly depend on the location of the marked node.

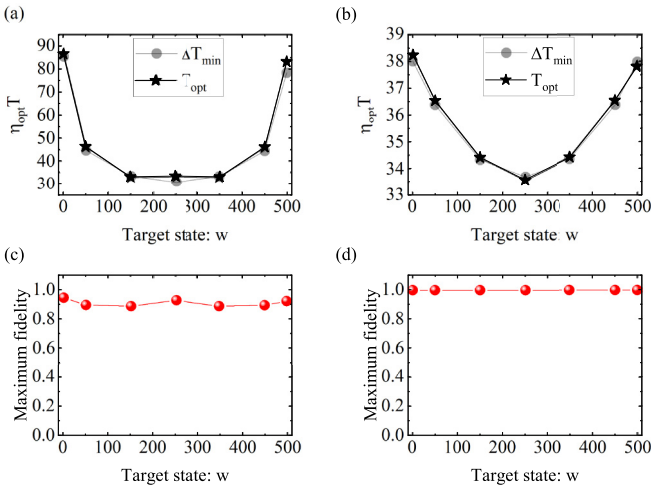

FIG. 3. Changes in search time and fidelity when selecting different target states, taking $n = 500$ as an example for target states $w = 1$, 50, 150, 250, 350, 450, 499. (a) and (c) Multiple-power-law interactions in 1D optical lattices and (b) and (d) exponentially decaying interactions in the waveguide-QED system.

IV. QUANTUM SEARCH WITH A NOISE EFFECT

In the previous section, we investigated the quantum search in three different physical systems and showed that a near quadratic speedup can be realized in all three cases without considering the dissipation effects. However, in real physical systems dissipations, including decay and dephasing, need to be taken into account. Here, we consider the maximum fidelity (i.e., success probability) of the quantum search under decay and dephasing using two methods. The first one is based on the master equation, which is given by

$$\dot{\rho}_s(t) = -i[H_{\rm coh}, \rho_s(t)] + \mathcal{L}[\rho_s(t)], \tag{3}$$

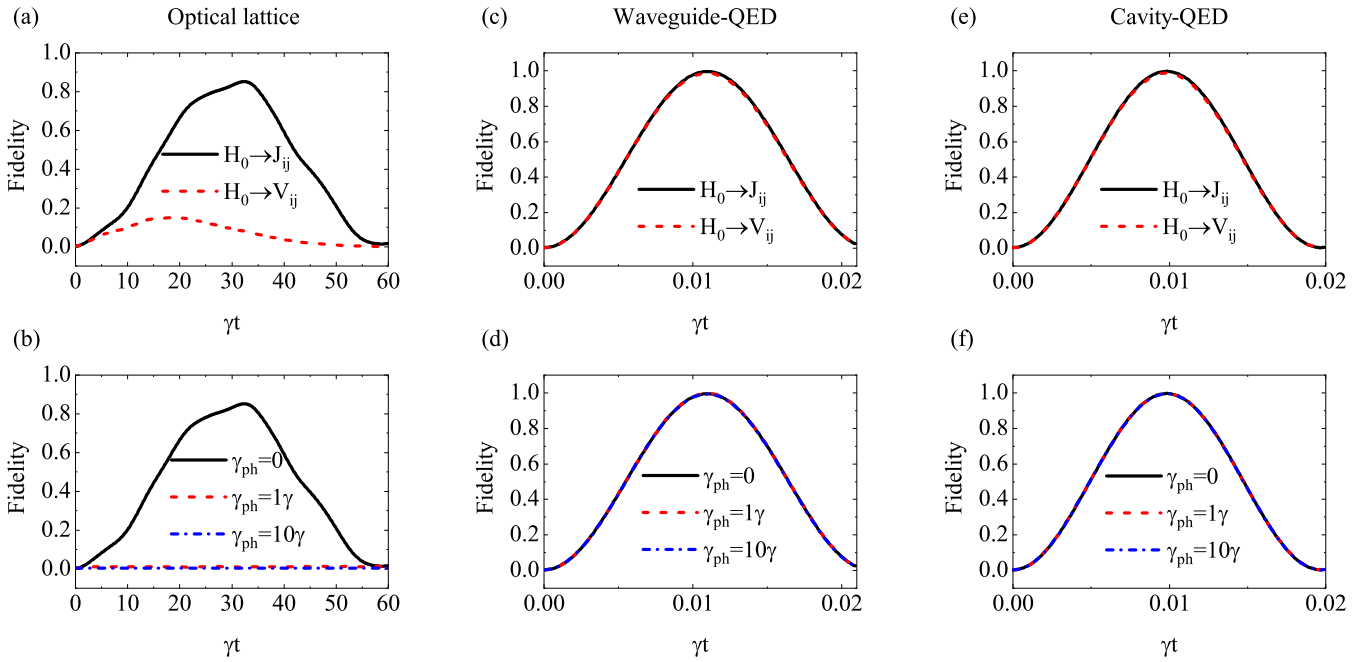

FIG. 4. Quantum search fidelity with dissipation effects. Free-space optical lattice with mixed-power-law interaction with (a) decay and (b) different dephasing rates. Waveguide-QED system with exponentially decaying interactions ($\Gamma = 20\gamma$ and $\kappa = 0.001$) with (c) collective decay and (d) different dephasing rates. Cavity-QED system with ideal long-range interaction ($J_{ij} = 10\gamma$) under (e) decay and (f) different dephasing rates. Number of atoms $n = 256$.

where $H_{\rm coh} = \sum_{i<j} J_{ij}(|i\rangle\langle j| + |j\rangle\langle i|) + \eta H_t$ is the coherent part of the search Hamiltonian and the dissipation is captured by the Lindblad term $\mathcal{L}[\rho_s(t)]$. For the decay process, $\mathcal{L}[\rho_s(t)] = -\frac{1}{2}\sum_{ij}\Gamma_{ij}[\sigma_i^+\sigma_j^-\rho_s(t) + \rho_s(t)\sigma_i^+\sigma_j^- - 2\sigma_j^-\rho_s(t)\sigma_i^+]$, and for the dephasing process $\mathcal{L}[\rho_s(t)] = -\frac{\gamma_{\rm ph}}{2}\sum_j[\sigma_j^z\sigma_j^z\rho_s(t) + \rho_s(t)\sigma_j^z\sigma_j^z - 2\sigma_j^z\rho_s(t)\sigma_j^z]$, with $\gamma_{\rm ph}$ being the dephasing rate. The second method is to evolve the system under the effective search Hamiltonian $H_s = \sum_{ij}(J_{ij} + i\Gamma_{ij}/2))|i\rangle\langle j| + \eta H_t$, where the collective decay process has been included via the $i\Gamma_{ij}/2$ terms (see Table I). For the dephasing process, we can model the system by adding random local field fluctuations to the diagonal elements of the system Hamiltonian. These local fluctuations are not static and randomly fluctuate with time. For each time step of the evolution, we randomly generate a small fluctuation for each qubit; these fluctuations are sampled from a Gaussian distribution whose mean is zero, and the standard deviation is set by the dephasing rate $\gamma_{\rm ph}$ [44]. By running the quantum search many times (e.g., 500 times in our simulation), the results can be obtained by averaging over all the outputs. We compare the results using these two methods and find that they are consistent with each other (see Fig. 5 in the Appendix). This indicates the validity of using the effective Hamiltonian. Since the method based on the master equation is very time-consuming, here, we mainly use the method based on the effective Hamiltonian to evaluate the performance of our quantum search when $n > 100$.

The results are shown in Fig. 4, where the first row compares the search fidelity with and without the decay process and the second row shows the search fidelity under different dephasing rates. In Figs. 4(a), 4(c), and 4(e), the solid black line represents the case without decay, and the dotted red line represents the case considering decay. For the free-space optical lattice, the decay rate has a significant impact on the search fidelity; the maximum fidelity becomes very small when the decay is considered [Fig. 4(a)]. In contrast, the fidelities in the waveguide-QED system and the cavity-QED system with decay are almost the same as those without decay [Figs. 4(c) and 4(e)]. The main reason is that the energy gaps in these two systems are very large due to the enhanced atom-atom interaction and the time required for the quantum search is very short, which can significantly suppress the effect of dissipation. Similar phenomena also occur with dephasing. In Figs. 4(b), 4(d), and 4(f), we compare the search fidelity for three different dephasing rates ($\gamma_{\rm ph} = 0, 1\gamma$, and 10γ). We clearly see that dephasing can also significantly reduce the search fidelity in the free-space optical lattice system, while it has little effect in the other two systems. Thus, both the atom chain dispersively coupled to the cavity and the waveguide-QED system within the band gap are better candidate systems for realizing the optimal quantum search due to the enhanced long-range atom-atom interactions.

V. SUMMARY

We investigated the quantum spatial search problem in three different physical systems, i.e., an atom array trapped in an optical lattice, an atom array coupled to a 1D waveguide within the band gap, and atom arrays dispersively coupled to a good cavity. We found that close to quadratic speedup in the quantum search can be achieved in all three systems when there are no dissipations. However, when there are dissipations, including decay and dephasing, the waveguide-QED

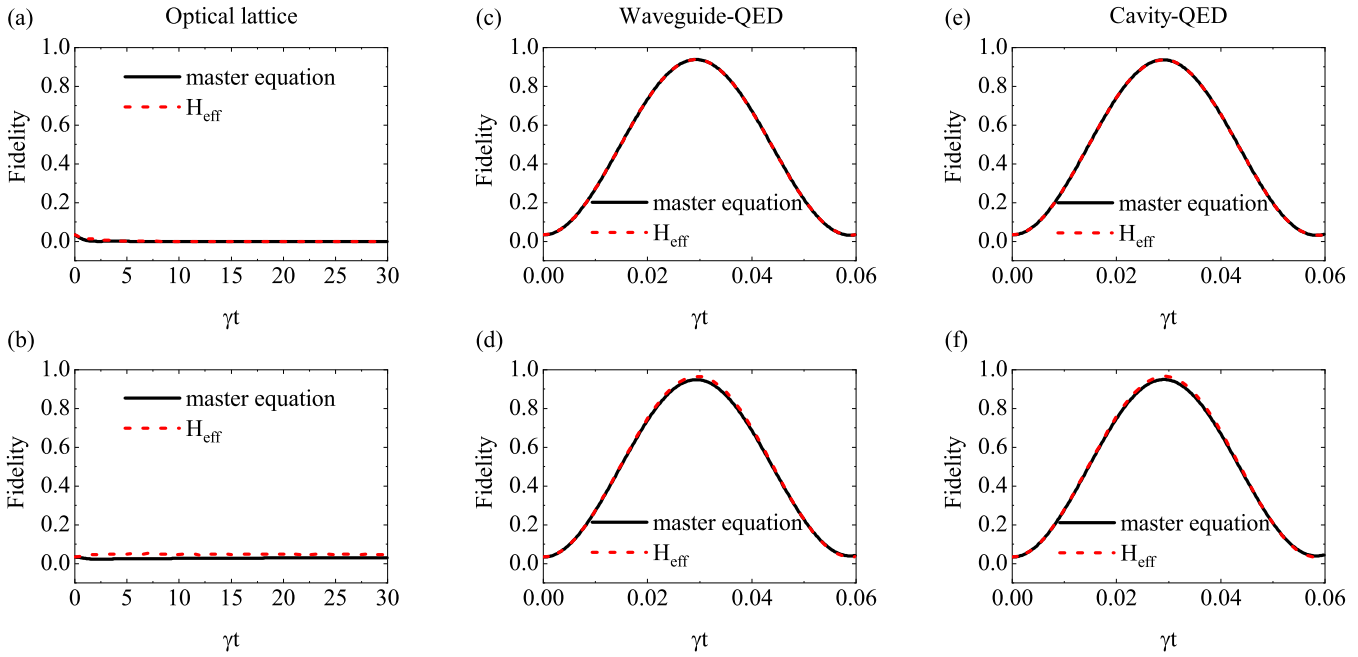

FIG. 5. The search fidelity with dissipation effects calculated using the master-equation method and effective Hamiltonian method with collective decay (top row) and with pure dephasing $\gamma_{\rm ph} = 1\gamma$ (bottom row) for (a) and (b) the optical lattice, (c) and (d) the waveguide-QED system, and (e) and (f) the cavity-QED system. Other parameters are $n = 30$ and $w = 8$.

and cavity-QED systems with enhanced collective interaction can still provide quadratic speedup with high success probability, while the success probability in the atom array trapped in an optical lattice is extremely low. These results indicate that the waveguide-QED and cavity-QED systems with long-range atom-atom interaction are better systems for demonstrating the optimal quantum search if the noise effect is considered. This is because the atom-atom interactions in the waveguide-QED and cavity-QED systems can be much larger than those in the free-space case even if two atoms are far apart in space. The enhanced collective long-range atom-atom interaction can result in a much larger spectral gap, which can significantly reduce the search time and suppress the effects of dissipation. Our results here can provide helpful instructions for realizing quantum search in real physical systems in the NISQ era.

ACKNOWLEDGMENTS

This work was supported by the National Key R&D Program of China (Grant No. 2021YFA1400800), the Key Program of National Natural Science Foundation of China (Grant No. 12334017), the Key-Area Research and Development Program of Guangdong Province (Grant No. 2018B030329001), the Guangdong Basic and Applied Basic Research Foundation (Grant No. 2023B1515040023), and the Natural Science Foundations of Guangdong (Grant No.2021A1515010039).

APPENDIX: TWO METHODS FOR CALCULATING THE DISSIPATION EFFECTS

The dissipation effects, including the decay and dephasing processes, can be accounted for either by the Lindblad-form master equation or the effective Hamiltonian methods, as illustrated in Sec. IV. Here, we compare the results of these two methods.

We take the number of atoms to be $n = 30$ and the target state to be $w = 8$ as an example. The results for the search fidelity using both the master-equation and the effective Hamiltonian methods are shown in Fig. 5, where the top row presents the results with decay while the bottom row presents the results with dephasing. We clearly see that the fidelities obtained with these two methods are almost the same for both the decay and dephasing processes. These results confirm the validity of the method using the effective Hamiltonian. Since the method using the master equation is very time-consuming and we can calculate only the cases with tens of atoms, we mainly use the method based on the effective Hamiltonian to calculate the performance of our search algorithm, especially when the number of atoms is greater than 100.

[1] M. A. Nielsen and I. L. Chuang, *Quantum Computation and Quantum Information* (Cambridge University Press, Cambridge, 2010).

[2] D. E. Knut, The art of computer programming, *Sorting and Searching* (Addison-Wesley, Reading, MA, 1973), Vol. 3, p. 736.

[3] L. K. Grover, A fast quantum mechanical algorithm for database search, in *Proceedings of the Twenty-Eighth Annual ACM Symposium on Theory of Computing, STOC '96* (Association for Computing Machinery, New York, 1996), pp. 212–219.

[4] L. K. Grover, Quantum mechanics helps in searching for a needle in a haystack, Phys. Rev. Lett. **79**, 325 (1997).

[5] L. K. Grover, Quantum computers can search rapidly by using almost any transformation, Phys. Rev. Lett. **80**, 4329 (1998).

[6] G. L. Long, Grover algorithm with zero theoretical failure rate, Phys. Rev. A **64**, 022307 (2001).

[7] G. Li and L. Li, Deterministic quantum search with adjustable parameters: Implementations and applications, Inf. Comput. **292**, 105042 (2023).

[8] Y. Huang and S. Pang, Optimization of a probabilistic quantum search algorithm with a priori information, Phys. Rev. A **108**, 022417 (2023).

[9] A. N. Chowdhury and R. D. Somma, Quantum algorithms for Gibbs sampling and hitting-time estimation, Quantum Inf. Comput. **17**, 41 (2017).

[10] L. Lin and Y. Tong, Near-optimal ground state preparation, Quantum **4**, 372 (2020).

[11] A. A. Armenakas and O. K. Baker, Implementation and analysis of quantum computing application to Higgs boson reconstruction at the large Hadron Collider, Sci. Rep. **11**, 22850 (2021).

[12] R. D. Somma, S. Boixo, H. Barnum, and E. Knill, Quantum simulations of classical annealing processes, Phys. Rev. Lett. **101**, 130504 (2008).

[13] A. Lucas, Ising formulations of many NP problems, Front. Phys. **2**, 5 (2014).

[14] C. S. Yoon, C. H. Hong, M. S. Kang, J.-W. Choi, and H. J. Yang, Quantum asymmetric key crypto scheme using Grover iteration, Sci. Rep. **13**, 3810 (2023).

[15] N. J. Cerf, L. K. Grover, and C. P. Williams, Nested quantum search and structured problems, Phys. Rev. A **61**, 032303 (2000).

[16] K. Kastella and R. S. Conti, Signal enhancement and background suppression using interference and entanglement, Phys. Rev. A **83**, 014302 (2011).

[17] E. Farhi, J. Goldstone, S. Gutmann, J. Lapan, A. Lundgren, and D. Preda, A quantum adiabatic evolution algorithm applied to random instances of an NP-complete problem, Science **292**, 472 (2001).

[18] J. Roland and N. J. Cerf, Quantum search by local adiabatic evolution, Phys. Rev. A **65**, 042308 (2002).

[19] X. Peng, Z. Liao, N. Xu, G. Qin, X. Zhou, D. Suter, and J. Du, Quantum adiabatic algorithm for factorization and its experimental implementation, Phys. Rev. Lett. **101**, 220405 (2008).

[20] H. Hu and B. Wu, Optimizing the quantum adiabatic algorithm, Phys. Rev. A **93**, 012345 (2016).

[21] Y. Aharonov, L. Davidovich, and N. Zagury, Quantum random walks, Phys. Rev. A **48**, 1687 (1993).

[22] A. Nayak and A. Vishwanath, Quantum walk on the line, arXiv:quant-ph/0010117.

[23] J. Kempe, Quantum random walks: An introductory overview, Contemp. Phys. **44**, 307 (2003).

[24] R. Portugal, *Quantum Walks and Search Algorithms* (Springer, New York, 2013), Vol. 19.

[25] D. Lu, J. Zhu, P. Zou, X. Peng, Y. Yu, S. Zhang, Q. Chen, and J. Du, Experimental implementation of a quantum random-walk search algorithm using strongly dipolar coupled spins, Phys. Rev. A **81**, 022308 (2010).

[26] C. Benedetti, D. Tamascelli, M. G. A. Paris, and A. Crespi, Quantum spatial search in two-dimensional waveguide arrays, Phys. Rev. Appl. **16**, 054036 (2021).

[27] D. Qu, S. Marsh, K. Wang, L. Xiao, J. Wang, and P. Xue, Deterministic search on star graphs via quantum walks, Phys. Rev. Lett. **128**, 050501 (2022).

[28] E. Farhi and S. Gutmann, Analog analogue of a digital quantum computation, Phys. Rev. A **57**, 2403 (1998).

[29] A. M. Childs, E. Deotto, E. Farhi, J. Goldstone, S. Gutmann, and A. J. Landahl, Quantum search by measurement, Phys. Rev. A **66**, 032314 (2002).

[30] N. Shenvi, J. Kempe, and K. B. Whaley, Quantum random-walk search algorithm, Phys. Rev. A **67**, 052307 (2003).

[31] A. M. Childs and J. Goldstone, Spatial search by quantum walk, Phys. Rev. A **70**, 022314 (2004).

[32] E. Agliari, A. Blumen, and O. Mülken, Quantum-walk approach to searching on fractal structures, Phys. Rev. A **82**, 012305 (2010).

[33] L. Novo, S. Chakraborty, M. Mohseni, H. Neven, and Y. Omar, Systematic dimensionality reduction for quantum walks: Optimal spatial search and transport on non-regular graphs, Sci. Rep. **5**, 13304 (2015).

[34] S. Chakraborty, L. Novo, A. Ambainis, and Y. Omar, Spatial search by quantum walk is optimal for almost all graphs, Phys. Rev. Lett. **116**, 100501 (2016).

[35] S. Chakraborty, L. Novo, S. Di Giorgio, and Y. Omar, Optimal quantum spatial search on random temporal networks, Phys. Rev. Lett. **119**, 220503 (2017).

[36] T. Osada, B. Coutinho, Y. Omar, K. Sanaka, W. J. Munro, and K. Nemoto, Continuous-time quantum-walk spatial search on the Bollobás scale-free network, Phys. Rev. A **101**, 022310 (2020).

[37] J. Malmi, M. A. C. Rossi, G. García-Pérez, and S. Maniscalco, Spatial search by continuous-time quantum walks on renormalized internet networks, Phys. Rev. Res. **4**, 043185 (2022).

[38] S. Chakraborty, L. Novo, and J. Roland, Optimality of spatial search via continuous-time quantum walks, Phys. Rev. A **102**, 032214 (2020).

[39] A. Ambainis, A. Gilyén, S. Jeffery, and M. Kokainis, Quadratic speedup for finding marked vertices by quantum walks, in *Proceedings of the 52nd Annual ACM SIGACT Symposium on Theory of Computing* (ACM, 2020), pp. 412–424.

[40] S. Apers, S. Chakraborty, L. Novo, and J. Roland, Quadratic speedup for spatial search by continuous-time quantum walk, Phys. Rev. Lett. **129**, 160502 (2022).

[41] D. A. Meyer and T. G. Wong, Connectivity is a poor indicator of fast quantum search, Phys. Rev. Lett. **114**, 110503 (2015).

[42] J. Janmark, D. A. Meyer, and T. G. Wong, Global symmetry is unnecessary for fast quantum search, Phys. Rev. Lett. **112**, 210502 (2014).

[43] A. M. Childs and Y. Ge, Spatial search by continuous-time quantum walks on crystal lattices, Phys. Rev. A **89**, 052337 (2014).

[44] D. Lewis, A. Benhemou, N. Feinstein, L. Banchi, and S. Bose, Optimal quantum spatial search with one-dimensional long-range interactions, Phys. Rev. Lett. **126**, 240502 (2021).

[45] A. Sørensen and K. Mølmer, Entanglement and quantum computation with ions in thermal motion, Phys. Rev. A **62**, 022311 (2000).

[46] D. Lewis, L. Banchi, Y. H. Teoh, R. Islam, and S. Bose, Ion trap long-range XY model for quantum state transfer and optimal spatial search, Quantum Sci. Technol. **8**, 035025 (2023).

[47] K. Bharti, A. Cervera-Lierta, T. H. Kyaw, T. Haug, S. Alperin-Lea, A. Anand, M. Degroote, H. Heimonen, J. S. Kottmann, T. Menke, W.-K. Mok, S. Sim, L.-C. Kwek, and A. Aspuru-Guzik, Noisy intermediate-scale quantum algorithms, Rev. Mod. Phys. **94**, 015004 (2022).

[48] L. Novotny and B. Hecht, *Principles of Nano-optics*, 2nd ed. (Cambridge University Press, Cambridge, 2012).

[49] A. S. Sheremet, M. I. Petrov, I. V. Iorsh, A. V. Poshakinskiy, and A. N. Poddubny, Waveguide quantum electrodynamics: Collective radiance and photon-photon correlations, Rev. Mod. Phys. **95**, 015002 (2023).

[50] N. Defenu, T. Donner, T. Macrì, G. Pagano, S. Ruffo, and A. Trombettoni, Long-range interacting quantum systems, Rev. Mod. Phys. **95**, 035002 (2023).

[51] Z. Ficek and S. Swain, *Quantum Interference and Quantum Coherence: Theory and Experiment* (Springer, New York, 2004).

[52] Z. Liao and M. S. Zubairy, Single-photon modulation by the collective emission of an atomic chain, Phys. Rev. A **90**, 053805 (2014).

[53] Z. Liao, X. Zeng, S.-Y. Zhu, and M. S. Zubairy, Single-photon transport through an atomic chain coupled to a one-dimensional nanophotonic waveguide, Phys. Rev. A **92**, 023806 (2015).

[54] T. Caneva, M. T. Manzoni, T. Shi, J. S. Douglas, J. I. Cirac, and D. E. Chang, Quantum dynamics of propagating photons with strong interactions: A generalized input–output formalism, New J. Phys. **17**, 113001 (2015).

[55] Z. Liao, H. Nha, and M. S. Zubairy, Dynamical theory of single-photon transport in a one-dimensional waveguide coupled to identical and nonidentical emitters, Phys. Rev. A **94**, 053842 (2016).

[56] F. Xing, Y. Lu, and Z. Liao, Quantum correlation propagation in a waveguide-QED system with long-range interaction, Opt. Express **30**, 22963 (2022).

[57] F. Xing, Z. Liao, and X.-H. Wang, Deterministic generation of arbitrary n-photon states in a waveguide-QED system, Phys. Rev. A **109**, 013718 (2024).

[58] R. G. Hulet, E. S. Hilfer, and D. Kleppner, Inhibited spontaneous emission by a Rydberg atom, Phys. Rev. Lett. **55**, 2137 (1985).

[59] E. Yablonovitch, Inhibited spontaneous emission in solid-state physics and electronics, Phys. Rev. Lett. **58**, 2059 (1987).

[60] E. Shahmoon and G. Kurizki, Nonradiative interaction and entanglement between distant atoms, Phys. Rev. A **87**, 033831 (2013).

[61] J. S. Douglas, H. Habibian, C.-L. Hung, A. V. Gorshkov, H. J. Kimble, and D. E. Chang, Quantum many-body models with cold atoms coupled to photonic crystals, Nat. Photon. **9**, 326 (2015).

[62] G. S. Agarwal, *Quantum Optics* (Cambridge University Press, Cambridge, 2012).

[63] D. J. Heinzen, J. J. Childs, J. E. Thomas, and M. S. Feld, Enhanced and inhibited visible spontaneous emission by atoms in a confocal resonator, Phys. Rev. Lett. **58**, 1320 (1987).

[64] D. Najer *et al.*, A gated quantum dot strongly coupled to an optical microcavity, Nature (London) **575**, 622 (2019).

[65] T. G. Wong, Spatial search by continuous-time quantum walk with multiple marked vertices, Quantum Inf. Process. **15**, 1411 (2016).

[66] J. M. Chávez-Garcia, F. Solgun, J. B. Hertzberg, O. Jinka, M. Brink, and B. Abdo, Weakly flux-tunable superconducting qubit, Phys. Rev. Appl. **18**, 034057 (2022).

[67] F. Jarisch and M. Zeppenfeld, State resolved investigation of Förster resonant energy transfer in collisions between polar molecules and Rydberg atoms, New J. Phys. **20**, 113044 (2018).

[68] S. J. Evered *et al.*, High-fidelity parallel entangling gates on a neutral-atom quantum computer, Nature (London) **622**, 268 (2023).